

Quantum criticality at the Chern-to-normal insulator transition

Yu Xue and Emil Prodan*

Department of Physics, Yeshiva University, New York, NY 10016, USA

(Dated: December 2, 2024)

Using the non-commutative Kubo formula for aperiodic solids [1–3] and a recently developed numerical implementation [4], we study the conductivity σ and resistivity ρ tensors as functions of Fermi level E_F and temperature T , for models of strongly disordered Chern insulators. The formalism enabled us to converge the transport coefficients at temperatures low enough to enter the quantum critical regime at the Chern-to-trivial insulator transition. We find that the ρ_{xx} -curves at different temperatures intersect each other at one single critical point, and that they obey a single-parameter scaling law with an exponent close to the universally accepted value for the unitary symmetry class. However, when compared with the established experimental facts on the plateau-insulator transition in the Integer Quantum Hall Effect, we find a universal critical conductance σ_{xx}^c twice as large, an ellipse rather than a semi-circle law, and absence of the quantized Hall insulator phase.

PACS numbers: 72.25.-b, 72.10.Fk, 73.20.Jc, 73.43.-f

The criticality at the localization-delocalization transition (LDT) is believed to be universal and entirely determined by the generic symmetries of the systems [5]. One manifestation of this universality is a common scaling exponent ν per generic symmetry class, describing the diverging behavior of the localization length ξ at the mobility edge: $\xi \sim (E_F - E_F^c)^{-\nu}$. This in turn leads to a temperature-scaling of the transport coefficients at LDT [6]:

$$\rho(E_F, T) = F\left((E_F - E_F^c)(T/T_0)^{-\kappa}\right), \quad \kappa = p/2\nu, \quad (1)$$

when combined with the concept of temperature-induced effective size introduced by Thouless [7], and with the single-parameter scaling hypothesis [8, 9]. In Eq.1, F is a system dependent function, T_0 is a reference temperature, and p is the dynamical exponent for dissipation. Besides these universal scaling laws, there are other interesting universal aspects of the LDT, such as the existence of a single critical point (as opposed to a line of critical points) for the unitary symmetry class, universal values of the critical transport coefficients and universal renormalization flow-diagrams of the transport coefficients with the temperature or with the system-size.

Such universal characteristics at the plateau-plateau (PPT) and plateau-insulator (PIT) transitions in the Integer Quantum Hall Effect (IQHE) have preoccupied the experimental [10–29] and theoretical [26, 30–39] condensed matter communities for decades, resulting in some of the best experimental data and computer simulations available for a quantum transition. With the discovery of Topological Insulators (TI) [40–47], the principles of universality will receive renewed scrutiny. The TIs have bulk extended states even in the presence of strong disorder [48], hence they are expected to display sharp LDTs. As such, the transport measurements at the transitions could be as clean and revealing as the ones in IQHE. The TIs can fall in different symmetry classes [49, 50] and, even within the same symmetry class, the

topological materials can be very different from one another [51, 52], thus providing the perfect laboratory to test the principles of universality. The computer simulations have already begun this process [53–64] (note that these are all zero-temperature finite-size scaling simulations). One question that received great attention from these works is if the scaling exponents of the symplectic models at the metal-to-normal insulator and at the metal-to-topological insulator are the same. So far, the answer seems to be affirmative.

Although there is a substantial experimental transport data for TIs, only recently the focused was fully tuned on the topological-to-non topological phase transition [65–67]. And even these experiments need to be further refined for the quantum criticality to be revealed. Traditionally, the experiment was always ahead of the theoretical simulations in this domain (see [39] for a discussion), but we strongly believe that this state of affairs will be soon reversed by the adoption of the non-commutative geometry program for aperiodic solids, initiated by Bellissard *et al* in the 90's [1–3]. For example, this natural formalism for treating disordered solids under magnetic fields enabled us to develop extremely accurate, stable and efficient simulations of the zero- and finite-temperature transport coefficients [4, 48, 68, 69], to a point where qualitative and quantitative agreement between experiment and simulation was possible for PIT in IQHE [39]. In this Letter, we announce several predictions on the quantum criticality at the Chern-to-normal insulator transition. On a broader note, we want to announce that the simulations based on the non-commutative Kubo formula can now provide real guidance, via accurate predictions, for the experiments on quantum criticality at the topological-to-non topological phase transition.

The search for possible Chern Insulator (CI) materials have intensified and several theoretical studies have already singled out possible CI candidates [70–80]. This

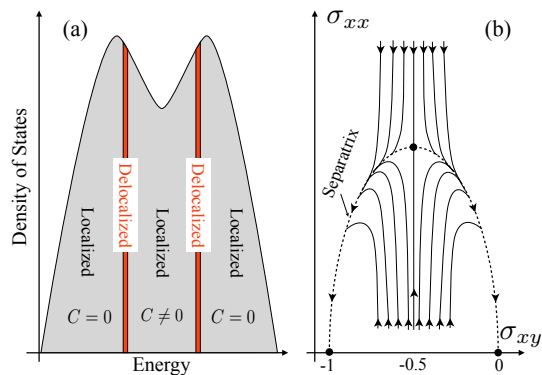


FIG. 1. (a) The spectrum of the disordered Chern insulator is localized everywhere except for two thin energy regions. (b) The expected flow of the transport coefficients when the temperature is lowered to zero. Different flow lines correspond to different Fermi levels. The dash line represents the separatrix, which is expected to satisfy a semi-circle law.

and the fact that the CIs and the IQHE liquids belong to the same unitary symmetry class motivated us to focus exclusively on CIs in this study. For the spin-up sector of the Kane-Mele (KM) [41] and of the Bernevig-Hughes-Zhang (BHZ) [43] models with strong disorder, we were able to converge (*i.e.* eliminate any finite-size effects) the finite-temperature conductivity σ and resistivity $\rho = \sigma^{-1}$ tensors, at temperatures low enough to enter the quantum critical regime at the transition between a CI and a normal insulator. We compare these results with the known facts for the PIT in IQHE [21, 23–26, 28, 81–84]. Like in PIT, the graphs of ρ_{xx} as function of electron density, recorded at different temperatures, intersect at one single critical point, and they collapse into a single curve after a single-parameter rescaling. The scaling exponent κ is in good agreement with what one would predict by using the universally accepted value of the finite-size scaling exponent $\nu = 2.6$ [58, 85–90] and with p fixed like in our simulations ($p = 1$). We clearly see the expected renormalization flow of σ with the temperature, but the separatrix is not a semicircle like at PIT, but rather an ellipse. At the critical point, we find $\sigma_{xy} \approx \frac{1}{2} \frac{e^2}{h}$ and, quite interestingly, $\sigma_{xx} \approx \frac{e^2}{h}$ rather than $\frac{1}{2} \frac{e^2}{h}$. The main surprise was, however, the absence of the Quantized Hall Insulator phase, characterized by $\sigma = 0$ but $\rho_{xy} = \frac{h}{e^2}$.

The key for our simulations is the non-commutative Kubo formula [1–3]:

$$\sigma_{ij}(E_F, T) = -\mathcal{T} \left([x_i, H] (1/\tau + \mathcal{L}_H)^{-1} [x_j, \Phi_{FD}(H)] \right), \quad (2)$$

where \mathcal{T} represents the trace over volume, H is the disordered Hamiltonian, x is the position operator, τ is the relaxation time for dissipation, \mathcal{L}_H is the Liouvillian and Φ_{FD} is the Fermi-Dirac distribution for a given T and E_F . In real condensed matter systems: $\tau \sim T^{-p}$, where p is the dynamical exponent appearing in Eq. 1. Eq. 2

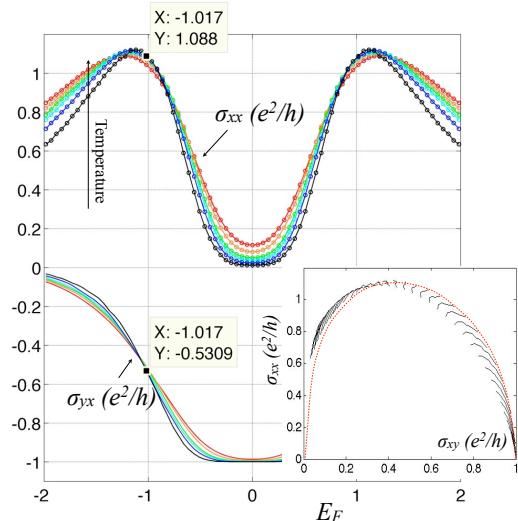


FIG. 2. σ as function of E_F at $kT = 1/\tau = 0.01, 0.02, 0.04, 0.06, 0.08$, simulated on an 80×80 lattice. For $T \geq 0.02$, this lattice-size is enough to virtually converge $\sigma^{(L)}$ while for $T = 0.01$ we start to see the finite-size effects. An average over many disorder configurations was considered (as many as 67 for $T = 0.01$ and 24 for $T = 0.08$). The marks posted on the graph give σ at the critical point. The inset shows the flow of our data in the $(\sigma_{xy}, \sigma_{xx})$ plane as $T \rightarrow 0$.

represents the thermodynamic limit of the formal Kubo formulas found in the solid state textbooks (see for example Eq. 3.385 and its finite-temperature version in [91]). It can be efficiently evaluated on a computer using a canonical finite-volume approximation [4], converging exponentially fast to the thermodynamic limit, a fact that was established with mathematical rigor. Extended discussions of the formalism, convergence tests and applications to the disordered Hofstadter model and to a disordered model of a quantum spin-Hall insulator can be found in Refs. [4, 39, 69].

We defer the analysis of the spin-up sector of the BHZ model to the supporting material, and here we present only the results for the spin-up sector of the KM model (no Rashba interaction), tuned in the middle of the CI topological phase:

$$H_0 = \sum_{\langle nm \rangle} |n\rangle \langle m| + 0.6i \sum_{\langle\langle nm \rangle\rangle} \tilde{\sigma}_n (|n\rangle \langle m| - |m\rangle \langle n|). \quad (3)$$

Here, $\tilde{\sigma}_n$ represents the isospin of the site n of the honeycomb lattice, and $\langle\rangle/\langle\langle\rangle\rangle$ symbolize first/second nearest neighbors. We add the random potential $V_\omega = W \sum_n \omega_n |n\rangle \langle n|$ to H_0 , where the ω 's are independent random variables uniformly distributed in $[-\frac{1}{2}, \frac{1}{2}]$. We fix $W = 4$ ($= 2 \times$ the clean insulating gap), in order to achieve the strong disorder regime where the insulating (spectral) gap is closed and only a mobility gap remains. The simulations are performed on a finite-size lattice containing 80×80 unit cells. By repeating the simulations

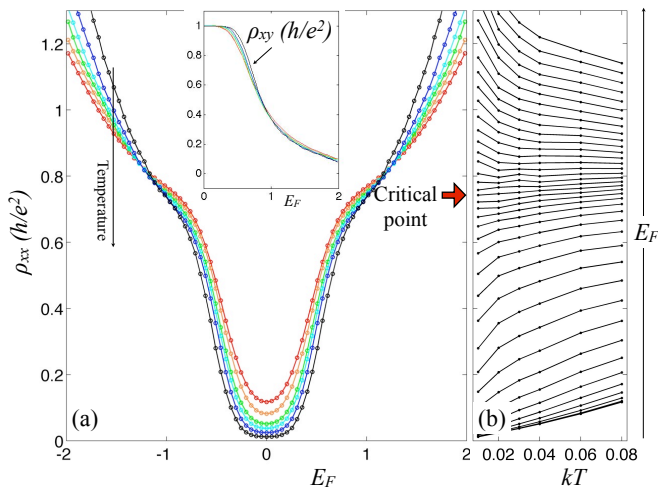


FIG. 3. (a) ρ_{xx} (and ρ_{xy} in the inset) as function of E_F at $kT = 0.01, 0.02, 0.04, 0.06$ and 0.08 . (b) ρ_{xx} as function of temperature for various E_F values. The arrow indicates the transition from CI to the normal insulator.

with different lattice sizes, we concluded that the effects due the finite-size of the simulation box are practically negligible for the temperatures considered in the present study (the effective Thouless length [7] is smaller than the simulation box).

In the above conditions, all the quantum states of the model are localized, except for the states in two narrow energy regions separating the CI from the normal insulator (see Fig. 1a). The existence of such delocalized quantum states can be demonstrated [48] with mathematical rigor using the theory of non-commutative Chern number [1], while numerically, it has been demonstrated using recursive Green's function and transfer matrix calculations [55, 73, 92, 93], level statistics analysis [48, 68, 94], simulations of the edge currents and computations of the edge conductance [95–97]. Near the transitions, the field-theoretic arguments developed by Pruisken and collaborators [98–101] for the IQHE predict the T -driven flow-diagram shown in Fig. 1(b), which was observed and confirmed in IQHE by experiment [11, 102].

The simulated σ is reported in Fig. 2 as function of Fermi level, for $kT = 1/\tau = 0.01, 0.02, 0.03, 0.04, 0.06$ and 0.08 (hence we fix $p = 1$ in our simulations). In this figure we can see an energy region where, especially for the lower temperatures, σ_{yx} takes the quantized value of -1 , indicating that the system is in the CI phase. When moving away from this energy region, σ_{yx} starts to converge towards 0 , indicating that the system enters the normal insulator phase. The σ_{yx} -curves computed at different temperatures intersect each other at practically one point. Examining the data for the direct conductivity, we see σ_{xx} decreasing with T for most part of the energy spectrum, a hallmark of the insulating phase, with the exception of two distinct energy regions where

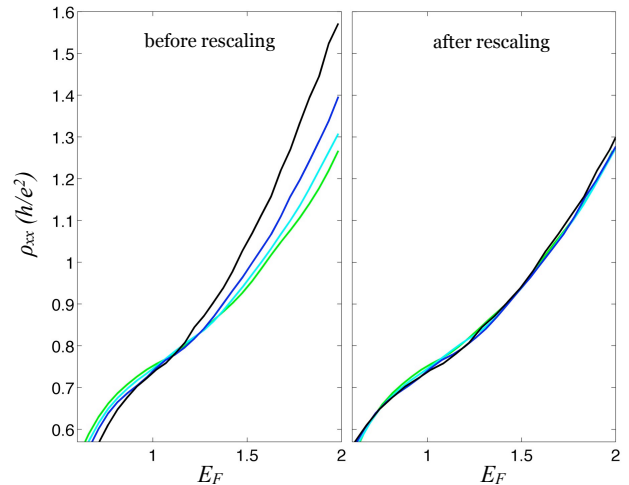


FIG. 4. ρ_{xx} at different temperatures collapses onto a single curve after the single-parameter rescaling: $E_F \rightarrow E_F^c + (E_F - E_F^c)(T/T_0)^{-\kappa}$, with $E_F^c = 1.017$, $T_0 = 0.04$ and $\kappa = 0.21$.

σ_{xx} increases with the temperature. These energy regions appear exactly where σ_{yx} switches between its quantized values and, as such, they must harbor extended quantum states [1]. The energy regions where σ_{xx} increases with T appear to become smaller and smaller as T is lowered, and that the maximum value of σ_{xx} stabilizes at a finite value (as opposed to diverging to infinity). An important question is if these regions reduce to a point as $T \rightarrow 0$. A more refined analysis based on Fig. 3 shows that this is indeed the case, and gives the critical Fermi levels $E_F^c \approx \pm 1.02$. The values of σ at E_F^c are marked in Fig. 2 and are $\sigma_{xx}^c \approx \frac{e^2}{h}$ and $\sigma_{xy}^c \approx \frac{1}{2} \frac{e^2}{h}$. These critical values for the conductance are reproduced when the simulations are repeated for the spin-up sector of the BHZ model. Furthermore, the PIT is known to exhibit a universal critical conductance [22], though with different values, so we are led to conjecture that the Chern-to-normal insulator transition also exhibits a universal conductance, with the universal values stated above.

When the data points from the main plot in Fig. 2 are placed in the $(\sigma_{xy}, \sigma_{xx})$ plane, we obtain the flow-diagram shown in the inset of Fig. 2. The separatrix for this flow, marked with the dotted line, has the shape of a semi-ellipse with the semi-axes $\frac{1}{2} \frac{e^2}{h}$ and $\frac{e^2}{h}$. At PIT in the IQHE, the separatrix strictly obeys the semicircle law: $\sigma_{xx}^2 + (\sigma_{xy} - 0.5e^2/h)^2 = (0.5e^2/h)^2$ [23]. Let us point out that the values $\sigma_{xy} > 0.5$ occur when E_F is located inside the old clean insulating gap, while the values $\sigma_{xy} < 0.5$ occur when E_F is located in the high-density spectrum resulted from the localization of the clean energy bands. As such, the flow (as $T \rightarrow 0$) starts from the inside (outside) of the ellipse and moves towards the separatrix for $\sigma_{xy} > 0.5$ ($\sigma_{xy} < 0.5$), a markedly different behavior when compared with PIT.

The existence of a unique critical point (as opposed to a line of critical points) at the Chern-to-normal transition can be established with great confidence by examining the resistivity tensor, plotted in Fig. 3. From the expression $\rho_{xx} = \sigma_{xx}/(\sigma_{xx}^2 + \sigma_{xy}^2)$, it follows that $\rho_{xx} \rightarrow 0$ inside the CI phase, while $\rho_{xx} \rightarrow \infty$ inside the normal insulating phase, when $T \rightarrow 0$. As a consequence, the ρ_{xx} -curves at different T must cross each other, very much like the σ_{yx} -curves do in Fig. 2. Since the plots are symmetric relative to the zero energy, we can focus only on the positive energies. Fig. 3(a) strongly suggests that all ρ_{xx} -curves cross each other at a single point, exactly how it was observed at PIT. To accurately pin-point this crossing point, we replotted ρ_{xx} in Fig. 3(b), this time as a function of temperature, for each positive E_F -value appearing in Fig. 3(a). The flow of ρ_{xx} with T curves down at lower E_F 's and it curves up at higher E_F 's. There is a clear separatrix between these two distinct tendencies, very much like in the experimental data on the PI transition in Ref. [103], or on the metal-insulator transition in Ref. [104]. This enables us to accurately identify the critical point: $E_F^c = \pm 1.017$, and then to determine the value of the conductivity tensor at the critical point: $\sigma_{xy}^c = -0.53 \times \frac{e^2}{h}$ and $\sigma_{xx}^c = 1.09 \times \frac{e^2}{h}$.

The inset in Fig. 3(a) reports $\rho_{xy} = \sigma_{yx}/(\sigma_{xx}^2 + \sigma_{xy}^2)$ as a function of E_F , which decreases from 1 to 0 almost with the same rate as σ_{yx} . As one can see, there is absolutely no tendency for ρ_{xy} to stay quantized at $\frac{h}{e^2}$ through the transition or further into the normal insulating phase. Such quantization of ρ_{xy} would have been incompatible with the critical values of σ determined above. It is also known that a quantized ρ_{xy} is equivalent with the semi-circle law [24], but the separatrix shown in the inset of Fig. 2 has an elliptical shape quite different from a semi-circle. We want to point out that these facts are also true for the simulations with the BHZ model. As such, we can conclude with great confidence that the quantized Hall insulator phase is absent for this system. This is in striking contrast with the PIT in IQHE, for which we did observe the quantized Hall insulating phase [39].

We now zoom into the region around E_F^c and start the scaling analysis. Since the scaling occur in the asymptotic limit $T \rightarrow 0$, we keep for this analysis only the lowest four temperatures. As shown in Fig. 4, the ρ_{xx} -curves collapse almost perfectly on top of each other after the energy axis is rescaled as: $E_F \rightarrow E_F^c + (E_F - E_F^c)(kT/kT_0)^{-\kappa}$ ($kT_0 = 0.04$). The best overlap of the rescaled curves is obtained for $\kappa = 0.21 \pm 0.01$, a value that is in good agreement with $k = 0.192$ obtained from the expression $\kappa = p/(2\nu)$ with the universally accepted value $\nu = 2.6$, and $p = 1$ like in our simulations. For the BHZ model, the agreement is not as good, very likely because there we need simulations at lower temperatures.

In conclusion, the simulations based on the non-commutative Kubo formula and a recently developed

numerical implementation enabled us to converge the transport coefficients at temperatures low enough to enter the quantum critical regime at the Chern-to-normal insulator transition. When compared with the available experimental facts and our previous simulations for PIT in IQHE, the results on the two strongly disordered Chern insulator models show similarities but also important differences. The similarities include the existence of a single critical point, single-parameter scaling behavior and a scaling exponent consistent with the universally accepted value. Among the dissimilarities were the absence of the quantized Hall insulator phase, a universal critical value of $\sigma_{xx}^c \approx \frac{e^2}{h}$ instead of $\sigma_{xx}^c \approx \frac{1}{2} \frac{e^2}{h}$, and the violation of the semi-circle law.

ACKNOWLEDGMENTS

This work was supported by the U.S. NSF grants DMS-1066045 and DMR-1056168.

* prodan@yu.edu

- [1] J. Bellissard, A. van Elst, and H. Schulz-Baldes, *J. Math. Phys.* **35**, 5373 (1994)
- [2] H. Schulz-Baldes and J. Bellissard, *J. Stat. Phys.* **91**, 991 (1998)
- [3] H. Schulz-Baldes and J. Bellissard, *Rev. Math. Phys.* **10**, 1 (1998)
- [4] E. Prodan, *Appl. Math. Res. Express Advance Access*(2012), doi:10.1093/amrx/abs017
- [5] F. Evers and A. D. Mirlin, *Rev. Mod. Phys.* **80**, 1355 (2008)
- [6] A. Pruisken, *Phys. Rev. Lett.* **61**, 1297 (1988)
- [7] D. J. Thouless, *Phys. Rev. Lett.* **39**, 1167 (1977)
- [8] E. Abrahams, P. Anderson, D. Licciardello, and T. Ramakrishnan, *Phys. Rev. Lett.* **42**, 673 (1979)
- [9] P. W. Anderson, D. J. Thouless, E. Abrahams, and D. S. Fisher, *Phys. Rev. B* **22**, 3519 (1980)
- [10] H. P. Wei, D. C. Tsui, and A. M. M. Pruisken, *Phys. Rev. B* **33**, 1488 (1985)
- [11] S. Kawaji and J. Wakabayashi, *J. Phys. Soc. Jpn* **56**, 21 (1987)
- [12] H. P. Wei, D. C. Tsui, M. A. Paalanen, and A. M. M. Pruisken, *Phys. Rev. Lett.* **61**, 1294 (1988)
- [13] J. Wakabayashi, M. Yamane, and S. Kamaji, *J. Phys. Soc. Jpn.* **58**, 1903 (1989)
- [14] J. Wakabayashi, A. Fukaro, S. Kawaji, Y. Koike, and T. Fukase, *Surf. Sci.* **229**, 60 (1990)
- [15] S. Koch, R. J. Haug, K. v. Klitzing, and K. Ploog, *Phys. Rev. B* **43**, 6828 (1991)
- [16] V. T. Dolgoplov, A. A. Shashkin, B. K. Medvedev, and V. G. Mokerov, *Sov. Phys. JETP* **72**, 113 (1991)
- [17] S. Koch, R. J. Haug, K. v. Klitzing, and K. Ploog, *Phys. Rev. Lett.* **67**, 883 (1991)
- [18] H. P. Wei, S.Y.Lin, and D. C.Tsui, *Phys. Rev. B* **45**, 3926 (1992)
- [19] J. Wakabayashi, S. Kavraji, T. Goto, T. Fukase, and Y. Koike, *J. Phys. Soc. Jpn* **61**, 1691 (1992)
- [20] S. Koch, R. Haug, K. von Klitzing, and K. Ploog, *Surf. Sci.* **263**, 108 (1992)

- [21] B. W. Alphenaar and D. A. Williams, *Phys. Rev. B* **50**, 5795 (1994)
- [22] D. Shahar, D. C. Tsui, M. Shayegan, R. N. Bhatt, and J. Cunningham, *Phys. Rev. Lett.* **74**, 4511 (1995)
- [23] D. Shahar, M. Hilke, C. C. Li, D. C. Tsui, S. L. Sondhi, J. E. Cunningham, and M. Razeghi, *Solid State Commun.* **107**, 19 (1998)
- [24] M. Hilke, D. Shahar, S. H. Song, D. C. Tsui, Y. H. Xie, and D. Monroe, *Nature* **395**, 675 (1998)
- [25] R. T. F. van Schaijk, A. de Visser, S. M. Olsthoorn, H. P. Wei, and A. M. M. Pruisken, *Phys. Rev. Lett.* **84**, 1567 (2000)
- [26] E. Shimshoni, *Mod. Phys. Lett. B* **18**, 923 (2004)
- [27] W. Li, G. A. Csathy, D. C. Tsui, L. N. Pfeiffer, and K. W. West, *Phys. Rev. Lett.* **94**, 206807 (2005)
- [28] A. de Visser, L. A. Ponomarenko, G. Galistu, D. T. N. de Lang, A. M. M. Pruisken, U. Zeitler, and D. Maude, *J. Phys. Conference Series* **51**, 379 (2006)
- [29] W. Li, C. L. Vicente, J. S. Xia, W. Pan, D. C. Tsui, L. N. Pfeiffer, and K. W. West, *Phys. Rev. Lett.* **102**, 216801 (2009)
- [30] O. Entin-Wohlman, A. G. Aronov, Y. Levinson, and Y. Imry, *Phys. Rev. Lett.* **22**, 4094 (1995)
- [31] S. L. Sondhi, S. M. Girvin, J. P. Carini, and D. Shahar, *Rev. Mod. Phys.* **69**, 315 (1997)
- [32] D. N. Sheng and Z. Y. Weng, *Phys. Rev. B* **59**, R7821 (1999)
- [33] L. P. Pryadko and A. Auerbach, *Phys. Rev. Lett.* **82**, 1253 (1999)
- [34] D. N. Sheng and Z. Y. Weng, *Phys. Rev. B* **62**, 15363 (2000)
- [35] U. Zulicke and E. Shimshoni, *Physica E* **12**, 674 (2002)
- [36] P. Cain and R. A. Romer, *Europhys. Lett.* **66**, 104 (2004)
- [37] Y. Dubi, Y. Meir, and Y. Avishai, *Phys. Rev. Lett.* **94**, 156406 (2005)
- [38] R. Levy and Y. Meir, arXiv:1005.5245v2(2010)
- [39] J. Song and E. Prodan, arXiv:1301.5305(2013)
- [40] F. D. M. Haldane, *Phys. Rev. Lett.* **61**, 2015 (1988)
- [41] C. L. Kane and E. J. Mele, *Phys. Rev. Lett.* **95**, 226801 (2005)
- [42] C. L. Kane and E. J. Mele, *Phys. Rev. Lett.* **95**, 146802 (2005)
- [43] B. A. Bernevig, T. L. Hughes, and S.-C. Zhang, *Science* **314**, 1757 (2006)
- [44] M. Koenig, S. Wiedmann, C. Bruene, A. Roth, H. Buhmann, L. W. Molenkamp, X.-L. Qi, and S.-C. Zhang, *Science* **318**, 766 (2007)
- [45] J. E. Moore and L. Balents, *Phys. Rev. B* **75**, 121306 (2007)
- [46] L. Fu and C. L. Kane, *Phys. Rev. B* **76**, 045302 (2007)
- [47] D. Hsieh, D. Qian, L. Wray, Y. Xia, Y. S. Hor, R. J. Cava, and M. Z. Hasan, *Nature* **452**, 970 (2008)
- [48] E. Prodan, *J. Phys. A: Math. Theor.* **44**, 113001 (2011)
- [49] A. P. Schnyder, S. Ryu, A. Furusaki, and A. W. W. Ludwig, *Phys. Rev. B* **78**, 195125 (2008)
- [50] S. Ryu, A. P. Schnyder, A. Furusaki, and A. W. Ludwig, *New J. Phys.* **12**, 065010 (2010)
- [51] M. Z. Hasan and C. L. Kane, *Rev. Mod. Phys.* **82**, 3045 (2010)
- [52] X.-L. Qi and S.-C. Zhang, *Rev. Mod. Phys.* **83**, 1057 (2011)
- [53] Y. Asada, K. Slevin, and T. Ohtsuki, *Phys. Rev. B* **70**, 135115 (2004)
- [54] P. Markos and L. Schweitzer, *J. Phys. A: Math. Gen* **39**, 3221 (2006)
- [55] M. Onoda, Y. Avishai, and N. Nagaosa, *Phys. Rev. Lett.* **98**, 076802 (2007)
- [56] H. Obuse, A. Furusaki, S. Ryu, and C. Mudry, *Phys. Rev. B* **76**, 075301 (2007)
- [57] M. V. Medvedyeva, J. Tworzydło, and C. W. J. Beenakker, *Phys. Rev. B* **81**, 214203 (2010)
- [58] I. C. Fulga, F. Hassler, A. R. Akhmerov, and C. W. J. Beenakker, *Phys. Rev. B* **84**, 245447 (2011)
- [59] I. C. Fulga, F. Hassler, and A. R. Akhmerov, *Phys. Rev. B* **85**, 165409 (2012)
- [60] E. P. L. van Nieuwenburg, J. M. Edge, J. P. Dahlhaus, J. Tworzydło, and C. W. J. Beenakker, *Phys. Rev. B* **85**, 165131 (2012)
- [61] I. C. Fulga, A. R. Akhmerov, J. Tworzydło, B. Beri, and C. W. J. Beenakker, *Phys. Rev. B* **86**, 054505 (2012)
- [62] R. S. K. Mong, J. H. Bardarson, and J. E. Moore, *Phys. Rev. Lett.* **108**, 076804 (2012)
- [63] E. Rossi, J. H. Bardarson, M. S. Fuhrer, and S. D. Sarma, *Phys. Rev. Lett.* **109**, 096801 (2012)
- [64] A. Yamakage, K. Nomura, K.-I. Imura, and Y. Kuramoto, arXiv:1211.5026(2012)
- [65] T. Sato, K. Segawa, K. Kosaka, S. Souma, K. Nakayama, K. Eto, T. Minami, Y. Ando, and T. Takahashi, *Nature Phys.* **7**, 840 (2011)
- [66] S.-Y. Xu, Y. Xia, L. A. Wray, S. Jia, F. Meier, J. H. Dil, J. Osterwalder, B. Slomski, A. Bansil, H. Lin, R. J. Cava, and M. Z. Hasan, *Science* **332**, 560 (2011)
- [67] M. Brahlek, N. Bansal, N. Koirala, S.-Y. Xu, M. Neupane, C. Liu, M. Z. Hasan, and S. Oh, *Phys. Rev. Lett.* **109**, 186403 (2012)
- [68] E. Prodan, T. Hughes, and B. Bernevig, *Phys. Rev. Lett.* **105**, 115501 (2010)
- [69] Y. Xue and E. Prodan, *Phys. Rev. B* **86**, 155445 (2012)
- [70] C. Wu, *Phys. Rev. Lett.* **101**, 186 (2008)
- [71] J. Inoue and A. Tanaka, *Phys. Rev. Lett.* **105**, 017401 (2010)
- [72] G. Xu, H. Weng, Z. Wang, X. Dai, and Z. Fang, *Phys. Rev. Lett.* **107**, 186806 (2011)
- [73] Z. Xu, L. Sheng, D. Y. Xing, E. Prodan, and D. N. Sheng, *Phys. Rev. B* **85**, 075115 (2012)
- [74] A. M. Essin and V. Gurarie, *Phys. Rev. B* **85**, 195116 (2012)
- [75] H. Zhang, F. Freimuth, G. Bihlmayer, S. Blügel, and Y. Mokrousov, *Phys. Rev. B* **86**, 035104 (2012)
- [76] A. Rüegg, C. Mitra, A. A. Demkov, and G. A. Fiete, *Phys. Rev. B* **85**, 245131 (2012)
- [77] H. Li, L. Sheng, and D. Y. Xing, *Phys. Rev. B* **85**, 045118 (2012)
- [78] M. Ezawa, *Phys. Rev. Lett.* **109**, 055502 (2012)
- [79] M. Ezawa, *Phys. Rev. Lett.* **110**, 026603 (2013)
- [80] X.-L. Zhang, L.-F. Liu, and W.-M. Feng, arXiv:1301.4081(2013)
- [81] R. B. Dunforda, N. Griffin, M. Pepper, P. J. Phillips, and T. E. Whall, *Physica E* **6**, 297 (2000)
- [82] L. A. Ponomarenko, D. T. N. de Lang, A. de Visser, D. K. Maude, B. N. Zvonkov, R. A. Lunin, and A. M. M. Pruisken, *Physica E* **22**, 236 (2004)
- [83] A. Pruisken, D. de Lang, L. Ponomarenko, and A. de Visser, *Solid State Commun.* **137**, 540 (2006)
- [84] D. T. N. de Lang, L. A. Ponomarenko, A. de Visser, and A. M. M. Pruisken, *Phys. Rev. B* **75**, 035313 (2007)
- [85] K. Slevin and T. Ohtsuki, *Phys. Rev. B* **80**, 041304 (2009)
- [86] B. Kramer, A. MacKinnon, T. Ohtsuki, and K. Slevin, *Int. J. Mod. Phys. B* **24**, 1841 (2010)
- [87] H. Obuse, A. R. Subramaniam, A. Furusaki, I. A. Gruzberg, and A. W. W. Ludwig, *Phys. Rev. B* **82**, 035309 (2010)
- [88] J. P. Dahlhaus, J. M. Edge, J. Tworzydło, and C. W. J. Beenakker, *Phys. Rev. B* **84**, 115113 (2011)
- [89] M. Amado, A. V. Malyshev, A. Sedrakyan, and F. Domnguez-Adame, *Phys. Rev. Lett.* **107**, 066402 (2011)

- [90] K. Slevin and T. Ohtsuki, *Int. J. Mod. Phys.: Conference Series* **11**, 60 (2012)
- [91] G. D. Mahan, *Many-Particle Physics*, 3rd ed. (Springer, New York, 2000)
- [92] A. Yamakage, K. Nomura, K. I. Imura, and Y. Kuramoto, *J. Phys. Soc. Jpn.* **80**, 053703 (2011)
- [93] J. Song, H. Liu, H. Jiang, Q.-F. Sun, and X. C. Xie, *Phys. Rev. B* **85**, 195125 (2012)
- [94] V. Chua and G. A. Fiete, *Phys. Rev. B* **84**, 195129 (2011)
- [95] J. Li, R. L. Chu, J. K. Jain, and S. Q. Shen, *Phys. Rev. Lett.* **102**, 136806 (2009)
- [96] C. W. Groth, M. Wimmer, A. R. Akhmerov, J. Tworzydło, and C. W. J. Beenakker, *Phys. Rev. Lett.* **103**, 196805 (2009)
- [97] H. Jiang, L. Wang, Q. F. Sun, and X. C. Xie, *Phys. Rev. B* **80**, 165316 (2009)
- [98] A. M. M. Pruisken, *Nuc. Phys. B* **235**, 277 (1984)
- [99] H. Levine, S. B. Libby, and A. M. M. Pruisken, *Nucl. Phys. B* **240**, 30 (1984)
- [100] H. Levine, S. B. Libby, and A. M. M. Pruisken, *Nucl. Phys. B* **240**, 49 (1984)
- [101] H. Levine, S. B. Libby, and A. M. M. Pruisken, *Nucl. Phys. B* **240**, 71 (1984)
- [102] M. Yamane, J. Wakabayashi, and S. Kawaji, *J. Phys. Soc. Jpn.* **58**, 1899 (1989)
- [103] S. Q. Murphy, J. L. Hicks, W. K. Liu, S. J. Chung, K. J. Goldammer, and M. B. Santos, *Physica E* **6**, 293 (2000)
- [104] D. A. Knyazev, O. E. Omelyanovskii, V. M. Pudalov, and I. S. Burmistrov, *Phys. Rev. Lett.* **100**, 046405 (2008)

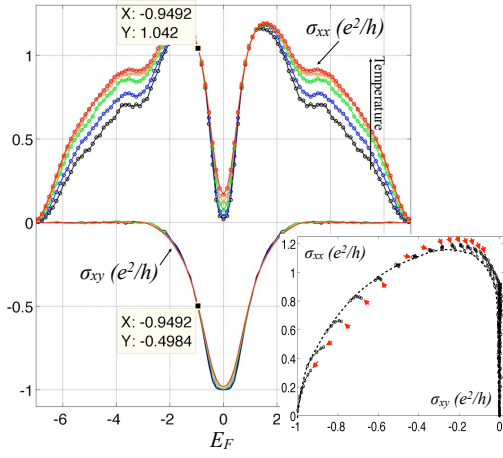


FIG. 5. The simulated σ as function of E_F at $kT = 1/\tau = 0.01, 0.02, 0.04, 0.06, 0.08$, simulated on an 80×80 lattice. The inset shows the T -driven renormalization flow of σ in the $(\sigma_{xy}, \sigma_{xx})$ plane.

QUANTUM CRITICALITY AT THE CHERN-TO-NORMAL INSULATOR TRANSITION: SUPPORTING MATERIAL

This supporting material reports the simulations based on the non-commutative Kubo formula, for the Chern Insulator (CI) corresponding to the spin-up sector of the Bernevig-Hughes-Zhang (BHZ) model [1] (tuned in the middle of the topological phase):

$$h(\mathbf{k}) = \sigma_x \sin k_x + \sigma_y \sin k_y + 2(1 + \cos k_x + \cos k_y)\sigma_z. \quad (4)$$

This model can be represented on a 2-dimensional square-lattice with two orbitals per site. The lattice sites are indexed by \mathbf{n} and the orbitals by α . In this real-space representation, we add the random potential $V_\omega = W \sum_{\mathbf{n}, \alpha} \omega_{\mathbf{n}, \alpha} c_{\mathbf{n}, \alpha}^\dagger c_{\mathbf{n}, \alpha}$, where $c_{\mathbf{n}, \alpha}^\dagger$ creates an electron in state α at site \mathbf{n} , and ω 's are independent random variables uniformly distributed in $[-1/2, 1/2]$. We fixed $W = 5$ ($= 2.5 \times$ the clean insulating gap), to achieve the strong disorder regime where the insulating gap is closed and only a mobility gap remains. The lattice size was taken to be 80×80 . An average over many disorder configurations was considered for different temperatures, specifically: 68 configurations for $kT = 0.01$, 67 for $kT = 0.02$, 23 for $kT = 0.04, 0.06$ and 0.08 . We want to point out that, in order to enter the full quantum critical regime, simulations at lower temperatures are needed for the present model.

Like in the main text, Fig. 5 reports the simulated conductivity tensor σ as function of Fermi level E_F , at various temperatures T . The inset shows the T -driven flow of σ in the $(\sigma_{xy}, \sigma_{xx})$ plane. A more refined analysis from Fig. 6 indicates a single critical point located at the critical Fermi level $E_F^c \approx 0.94$. The critical σ values at E_F^c were

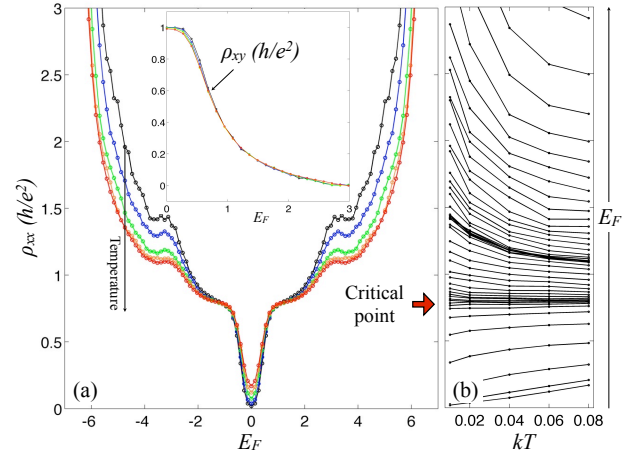


FIG. 6. (a) ρ_{xx} (and ρ_{xy} in the inset) as function of E_F at $kT = 0.01, 0.02, 0.04, 0.06$ and 0.08 . (b) ρ_{xx} as function of temperature for various E_F values. The arrow indicates the transition from CI to the normal insulator.

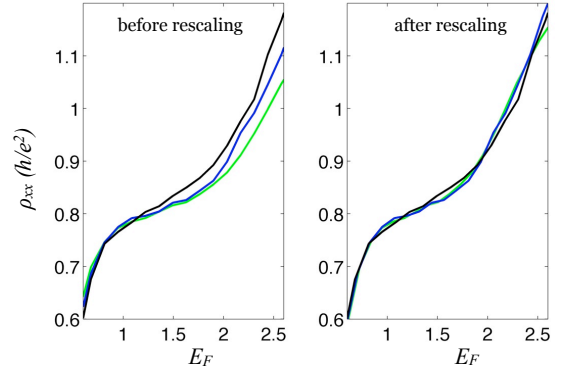


FIG. 7. Single-parameter rescaling: $E_F \rightarrow E_F^c + (E_F - E_F^c)(T/T_0)^{-\kappa}$, with $E_F^c = 0.94$, $T_0 = 0.01$ and $\kappa = 0.14$.

found to be $\sigma_{xx}^c \approx \frac{e^2}{h}$ and $\sigma_{xy}^c \approx \frac{1}{2} \frac{e^2}{h}$ (the exact values are marked on the graph).

Like in the main text, Fig. 6 reports the simulated resistivity tensor ρ (a) as function of E_F , at various temperatures, and (b) as function of kT , at various Fermi levels. The flow with T in Fig. 6(b) is used to determine the critical point. The inset shows no trace of the quantized Hall insulator phase.

Like in the main text, Fig. 7 reports the scaling analysis. Only the lowest temperatures have been considered. The best overlap of the rescaled curves is obtained for $\kappa = 0.14 \pm 0.01$. It is very likely that this value will improve when lower temperatures will be considered in the future.

-
- [1] B. A. Bernevig, T. L. Hughes, and S.-C. Zhang, *Science* **314**, 1757 (2006).

* prodan@yu.edu